

TW

**stichting
mathematisch
centrum**



AFDELING TOEGEPASTE WISKUNDE

TW 118/70

AUGUSTUS

M.P. VAN OUWERKERK-DIJKERS
SH-WAVES IN A HALF-SPACE WITH LINEARLY INCREASING
PROPAGATION VELOCITY

TW

2e boerhaavestraat 49 amsterdam

BIBLIOTHEEK MATHEMATISCH CENTRUM
 AMSTERDAM

Printed at the Mathematical Centre, 49, 2e Boerhaavestraat, Amsterdam.

The Mathematical Centre, founded the 11-th of February 1946, is a non-profit institution aiming at the promotion of pure mathematics and its applications. It is sponsored by the Netherlands Government through the Netherlands Organization for the Advancement of Pure Research (Z.W.O), by the Municipality of Amsterdam, by the University of Amsterdam, by the Free University at Amsterdam, and by industries.

Contents

1. Introduction.
2. Statement of the problem and formal solution.
3. Contour-integral method.
4. Saddle-point method.
5. The inverse Laplace transform.

References.

Appendix 1. Uniform asymptotic expansion of Bessel functions.

2. Poles of the solution for small $\zeta(0)$.
3. Calculation of the residues for small $\zeta(0)$.
4. The geometrical part of the solution.
5. Details of the saddle-point calculations.

1. Introduction

The problem of wave propagation in a stratified medium which contains a low-velocity layer has been studied fairly thoroughly in the case of acoustic waves in a fluid medium, e.g. SOFAR propagation [3], [5]. The related problem of long-distance radiowave propagation in the atmosphere has also been treated [3]. The associated phenomenon of elastic wave propagation in a solid medium, of interest to geophysicists, has been comparatively little investigated [2], [8].

In this report a study is made of the propagation of an SH-pulse emitted by a line source parallel to the free surface of a semi-infinite medium. The velocity of propagation increases linearly with the distance from the surface. Asymptotical methods are applied to an integral representation of the solution. Some of the results can be compared to those obtained from Keller's geometrical theory of diffraction [2], [6], which are given in an appendix. Some of the asymptotic irregularities encountered are directly related to those observed by Lapwood [7] (see also [9]). In those cases where analytical treatment would have been too complicated recourse has been taken to numerical methods. The computations were performed on the Electrologica X8 computer at the Mathematical Centre. Some of the figures were plotted by Mr. Haringhuizen and Mr. van der Horst using the Electrologica X1.

This work was begun at the Department of Applied Mathematics and Theoretical Physics of the University of Cambridge, Great Britain, at a suggestion of Dr. E.R. Lapwood. Discussions with him and his staff and later with Prof. Dr. H.A. Lauwerier were extremely helpful.

2. Statement of the problem and formal solution

Consider a semi-infinite inhomogeneous isotropic elastic medium occupying $z \geq 0$. A line source in the direction of the y -axis parallel to the free surface $z = 0$ emits an SH-pulse at the instant $t = 0$. The displacement U is independent of y and satisfies

$$(2.1) \quad \frac{1}{\mu} \nabla \cdot (\mu \nabla U) - \frac{1}{c^2} \frac{\partial^2 U}{\partial t^2} = -\delta(x) \delta(z-z_1) \delta(t),$$

where c is the velocity of propagation of SH-waves and μ is the rigidity of the medium. Both c and μ are functions of z only, i.e. $c = c_0(1+\alpha z)$ and $\mu = \mu_0(1+\alpha z)^p$, where the real positive constant α is small, c_0 , μ_0 are real and positive and p is arbitrary. At $z = 0$ we have $(\partial U / \partial z) = 0$, while the displacement tends to zero at infinity.

We apply the transformations $\tilde{U}(x, z; s) = \int_0^\infty e^{-st} U dt$ and $U^*(\xi, z; s) = \int_{-\infty}^\infty e^{-i\xi x} \tilde{U} dx$. Then U^* satisfies

$$(2.2) \quad \frac{1}{\mu} \frac{d}{dz} \left(\mu \frac{dU^*}{dz} \right) - [\xi^2 + \left(\frac{s}{c} \right)^2] U^* = -\delta(z-z_1)$$

with appropriate conditions at $z = 0$ and for $z \rightarrow \infty$.

This is equivalent to the following statement. U^* satisfies the homogeneous form of (2.2) almost everywhere, while at $z = z_1$

$$(2.3) \quad \left[U^* \right]_{z_1^-}^{z_1^+} = 0 \quad \text{and} \quad \left[\frac{dU^*}{dz} \right]_{z_1^-}^{z_1^+} = -1.$$

We introduce a new variable v and a new unknown function $V(v)$ by

$$(2.4) \quad v = \xi(1+\alpha z)/\alpha \quad \text{and} \quad U^* = \chi(v) V(v),$$

where $\chi(v) = (v/v_1)^{(1-p)/2}$ and $v_1 = \xi(1+\alpha z_1)/\alpha$.

Then $V(v)$ satisfies Bessel's equation almost everywhere, viz.

$$\frac{d^2 V}{dv^2} + \frac{1}{v} \frac{dV}{dv} - [1 + (\frac{N}{v})^2] V = 0,$$

where $N = [(\frac{s}{\alpha c_0})^2 + (\frac{p-1}{2})^2]^{\frac{1}{2}}$ and $\text{Re } N \geq 0$,

while $\left[\frac{V}{v} \right]_{v_1}^{v_1^+} = 0$ and $\left[\frac{dV}{dv} \right]_{v_1}^{v_1^+} = -\frac{1}{\xi}$,

$$\xi \frac{dV}{dv} + \alpha \frac{1-p}{2} V = 0 \quad \text{at } v = \xi/\alpha$$

and $|(v/v_1)^{(1-p)/2} V| \rightarrow 0$ as $|v| \rightarrow \infty$.

The transformed solution will be a combination of modified Bessel functions. We choose a combination V^+ which is unbounded as $z \rightarrow \infty$ and a combination V^- which tends to zero as $z \rightarrow \infty$. Now we can write the solution as

$$(2.5) \quad \begin{aligned} V &= C(V^+(v_1) - \frac{W^+}{W^-} V^-(v_1))V^-(v), & z \geq z_1, \\ &= C(V^+(v) - \frac{W^+}{W^-} V^-(v))V^-(v_1), & 0 \leq z \leq z_1, \end{aligned}$$

where $C = \frac{1}{\xi} (V^- \frac{dV^+}{dv} - V^+ \frac{dV^-}{dv})^{-1}$ evaluated at $z = z_1$,

while $W^\pm = (v \frac{dV^\pm}{dv} + \frac{1-p}{2} V^\pm)$ evaluated at $z = 0$.

Obviously the inverse transformations cannot be carried out analytically. We will use asymptotic methods for large $\text{Re } s$ to obtain information for small t , i.e. the arrival times of the different pulses. This is made easier by the introduction of two new variables v and w by $\xi = ivs$ and $v = iNw$. The inverse Fourier transform then reads

$$(2.6) \quad \tilde{U} = \frac{s}{2\pi i} \int_{-i\infty e^{-i\phi}}^{i\infty e^{-i\phi}} e^{-vsx} U^* dv, \quad \text{where } \phi = \arg s, \quad |\phi| < \pi/2.$$

As the solution is symmetric in x , we will confine our considerations to positive x . When we use contour integration in the complex v -plane, we only need a solution with the correct behaviour in $\text{Re } vs \geq 0$, viz.

$$\begin{aligned}
 (2.7) \quad & V^+ = J_N(Nw) \text{ and } V^- = H_N^{(1)}(Nw) \text{ with } C = -\frac{\pi}{2i} \frac{1+\alpha z_1}{\alpha} \text{ in } \text{Im } vs > 0, \\
 & V^+ = J_N(Nw) \text{ and } V^- = H_N^{(2)}(Nw) \text{ with } C = \frac{\pi}{2i} \frac{1+\alpha z_1}{\alpha} \text{ in } \text{Im } vs < 0.
 \end{aligned}$$

The function V is now known explicitly in the half plane $\text{Re } vs \geq 0$ with the exception of an arbitrarily small angle $|\arg(vs)| < \epsilon$ where V must make a continuous transition from the representation for $\text{Im } vs > 0$ to that for $\text{Im } vs < 0$. A similar phenomenon has been discussed by Lapwood [7]. When we perform the inverse Laplace transformation this must be taken into account (see section 5).

For large $\text{Re } s$ we can use Olver's uniform asymptotic expansions of the Bessel functions [10], see also appendix 1. In the following section we will use the approximation $N = (\frac{s}{\alpha c_0}) + O(s^{-1})$.

All calculations will be performed in the region $0 \leq z \leq z_1$ and in most cases only for $0 < \phi < \pi/2$. The results for $z \geq z_1$ follow immediately by interchanging z and z_1 , while for $-\pi/2 < \phi < 0$ the solutions for $\text{Im } vs > 0$ and for $\text{Im } vs < 0$ change parts.

Section 3 is devoted to the inverse Fourier transformation with the aid of contour integration. This method gives us information about the normal modes. In section 4 the saddle-point method is used which determines the first arrivals.

3. Contour-integral method

We consider integral (2.6). Integration is performed along

$v = v_0 e^{i\frac{\pi}{2} - i\phi}$, with $-\infty < v_0 < \infty$. By adding a half circle at infinity in $\text{Re } vs \geq 0$ this contour may be closed. This half circle doesn't contribute to the value of the integral except when $[x^2 + (z-z_1)^2]^{\frac{1}{2}} = 0$, i.e. in the source. The value of (2.6) is equal to the contributions of the enclosed singularities. The only singularities of U^* in $\text{Re } vs \geq 0$ are branch points and first order poles. Of course $v = 0$ is a branch point. The corresponding cut extends from $v = 0$ to infinity in the left-hand half plane, so that the contour can be closed without crossing it.

If we use Olver's expansions in terms of Airy functions (see appendix 1) this will be the only branch point. If we use the exponential expansions three other branch points appear, $v = v(z)$, $v(z_1)$, $v(0)$, where $v(z) = \alpha N[s(1+\alpha z)]^{-1} \approx [c_0(1+\alpha z)]^{-1}$. Loop integrals along the sides of the branch cuts however give a zero-contribution because the numerical values of the Bessel-function approximations on opposite sides of the cuts are equal.

From (2.5) and (2.6) we see that the poles of the integrand are the zeros of W^- . The value of the integral will equal the sum of the residues in these poles. Asymptotically

$$\begin{aligned} W^- \sim & - 2^{3/2} e^{\pm \pi i/3} N^{1/3} \left[\left(\frac{1-w^2}{\zeta} \right)^{1/4} \text{Ai}'(e^{\pm 2\pi i/3} N^{2/3} \zeta) + \right. \\ & + e^{\pm \pi i/3} \left(\frac{\zeta}{1-w^2} \right)^{1/4} \text{Ai}(e^{\pm 2\pi i/3} N^{2/3} \zeta) N^{-2/3} + \\ & \left. + (1 + |N^{2/3} \zeta|^{1/4}) \exp\left(\frac{2}{3} N \zeta^{3/2}\right) O(N^{-2/3}) \right]_{z=0}, \end{aligned}$$

where

$$\frac{2}{3} \zeta^{3/2}(z) = \int_w^1 \frac{(1-\beta^2)^{\frac{1}{2}}}{\beta} d\beta \quad \text{and} \quad w = \frac{vs}{\alpha N} (1+\alpha z) \sim vc(1+\alpha z).$$

Figure 1. The position of poles and saddle points in the v -plane.

The upper sign applies when $\text{Im } v_s > 0$, the lower when $\text{Im } v_s < 0$. In first approximation the zeros of the Airy-function derivative, which are negative and real, determine the zeros of W^- , which are therefore situated near the curve with $\arg \zeta(0) = \pm \frac{\pi}{3} - \frac{2\phi}{3}$ (see figure 1 and 5). According to Olver [10] an approximate expression for the k th zero of W^- is

$$(3.1) \quad N^{2/3} \zeta_k(0) = e^{\mp 2\pi i/3} a'_k + o(s^{-2/3}), \quad \text{where } \text{Ai}'(a'_k) = 0.$$

This expression can be easily obtained for small $\zeta_k(0)$, i.e. near $v = v(0)$, as is demonstrated in appendix 2.

The number of poles K which must be taken into account, i.e. when $0 < \phi < \pi/2$ those for which $\text{Im } v_s > 0$ and when $-\pi/2 < \phi < 0$ those for which $\text{Im } v_s < 0$ (see again figure 1), can be estimated in the extreme cases of small $\zeta_k(0)$ (small $|\phi|$) and of large $\zeta_k(0)$ (small $\frac{\pi}{2} - |\phi|$). For small $\zeta_k(0)$ and large k the curve through the poles can be described by

$$(3.2) \quad v_k = \frac{1}{c_0} [1 - 2^{-1/3} \zeta + o(\zeta^2)].$$

Here $\zeta = \zeta_k(0) = \left[\frac{3\pi}{2} (k-3/4) \left| \frac{\alpha c_0}{s} \right| e^{-i(\pi+\phi)} \right]^{2/3} [1 + o(k^{-4/3})]$ for continuous k .

This curve crosses $v = te^{-i\phi}$ at $k - 3/4 = \frac{2^{3/2}}{3\pi} \left[\frac{\sin \phi}{\sin(2\pi-\phi)/3} \right]^{3/2} \left| \frac{s}{\alpha c_0} \right|$. The number of zeros K will be

$$(3.3) \quad K = \text{entier} \left\{ \frac{2^{3/2}}{3\pi} \left[\frac{\sin \phi}{\sin(2\pi-\phi)/3} \right]^{3/2} \left| \frac{s}{\alpha c_0} \right| + \frac{3}{4} \right\}.$$

When $\zeta_k(0)$ and k are both large the zero-curve can be described by

$$(3.4) \quad v_k \sim \frac{2}{c_0} \exp [-i\pi(k-3/4) \left| \frac{\alpha c_0}{s} \right| e^{-i\phi} - 1]$$

and the number of included zeros K is

$$(3.5) \quad K = \text{entier} \left\{ \frac{\phi}{\pi \cos \phi} \left| \frac{s}{\alpha c_0} \right| + \frac{3}{4} \right\}.$$

Using Cauchy's theorem we may write

$$(3.6) \quad \tilde{U} = \frac{\pi i}{2} c_0 (1 + \alpha z_1) \times \frac{s}{\alpha c_0} \sum_{k=1}^K \tilde{R}_K,$$

$$\text{where} \quad \tilde{R}_K = \left[\frac{W^+}{(\partial W^- / \partial v)} e^{-vsx} H_N^{(1)}(Nw) H_N^{(1)}(Nw_1) \right]_{v=v_k}, \quad 0 < \phi < \pi/2,$$

$$= - \left[\frac{W^+}{(\partial W^- / \partial v)} e^{-vsx} H_N^{(2)}(Nw) H_N^{(2)}(Nw_1) \right]_{v=v_k}, \quad -\pi/2 < \phi < 0,$$

$$\text{and} \quad v_k = \frac{1}{c_0} \left[1 + 2^{-1/3} e^{+2\pi i/3} (-a'_k) \left(\frac{\alpha c_0}{s} \right)^{2/3} + o(s^{-4/3}) \right]$$

for small $\zeta_k(0)$.

Details of the calculations are given in appendix 3. The results are

$$(3.7) \quad i\tilde{R}_k \sim \frac{2^{-4/3}}{\pi^2 c_0} \left(\frac{\alpha c_0}{s} \right)^{5/3} \epsilon_0 \exp \left[-s\tau_0 + 2^{-1/3} e^{\pi i/3} (-a'_k) \delta_0 \left(\frac{s}{\alpha c_0} \right)^{1/3} - \frac{2\pi i}{3} \right] \cdot$$

$$\cdot [1 + o(s^{-1/3})], \quad 0 < \phi < \pi/2,$$

$$\text{where} \quad \epsilon_0 = \{ [(1 + \alpha z_1)^2 - 1]^{1/4} [(1 + \alpha z)^2 - 1]^{1/4} (-a'_k) \text{Ai}^2(a'_k) \}^{-1},$$

$$\alpha c_0 \tau_0 = \alpha x - i \left[\int_1^{(1 + \alpha z_1)} + \int_1^{(1 + \alpha z)} \right] \frac{(w^2 - 1)^{1/2}}{w} dw$$

$$\text{and} \quad \delta_0 = \alpha x - i [(1 + \alpha z_1)^2 - 1]^{1/2} - i [(1 + \alpha z)^2 - 1]^{1/2}.$$

$$\text{For large } \zeta_k(0) \quad v_k \sim \frac{2}{c_0} \exp \left[\frac{2}{3} (-a'_k)^{3/2} \left(\frac{\alpha c_0}{s} \right) - 1 \right]$$

$$\text{and} \quad \tilde{R}_k \sim \frac{1}{2\pi^2 c_0} \frac{\zeta_k^{1/2} w_k}{(-a'_k) \text{Ai}^2(a'_k)} \left(\frac{\alpha c_0}{s} \right)^{5/3} \cdot$$

$$\cdot \exp \left\{ - \frac{s}{\alpha c_0} [\alpha x w_k - 2 \int_{w_k}^1 \frac{(1 - w^2)^{1/2}}{w} dw + \ln(1 + \alpha z_1)(1 + \alpha z)] + \frac{5\pi i}{6} \right\}.$$

When $-\pi/2 < \phi < 0$ ($-\tilde{R}_K$) is the complex conjugate of the above forms.

The inverse Laplace transformation of the residues is performed in section 5.

4. Saddle-point method.

In a different approach we use the saddle-point method to evaluate integral (2.6). To do this we have to expand U^* in exponential series (appendix 5) and determine the saddle-point of the individual terms. These can only be situated on the positive real v -axis, $0 < v \leq v(z_1)$ (see figure 1). Obviously the expansion of U^* in the region surrounding $0 < v \leq v(z_1)$ determines the behaviour of the integral.

The saddle-point contributions correspond directly to the geometrical part of the solution (see appendix 4 and figure 4) and each contribution can be identified with a definite type of ray. The conditions for the existence of the saddle-points determine the regions in the x, z -plane where the corresponding types of ray exist.

Although we can obtain the complete geometrical solution in this way we lose information about other aspects of the problem. If we write $(W^-)^{-1}$ as an infinite sum of exponential functions the poles (i.e. the normal modes) are hidden. In the following we will only substitute the expansions of its constituents in W^- , but we will retain the result in the denominator, and obtain the solution in the vicinity of the source plus a "least-distance" criterium for the normal modes.

In the region of the saddle-points

$$(4.1) \quad \frac{s}{2\pi i} e^{-vsx} \tilde{U} \sim \sum_{j=1}^6 U_j^*$$

$$\text{with} \quad U_j^* = \frac{1}{4\pi i} c_0(1+\alpha z_1) \times g_j(v)(1-w_1^2)^{-1/4}(1-w^2)^{-1/4} e^{-sf_j(v)} \cdot [1 + O(s^{-1})]$$

and

$$g_1 = \bar{f}ig_2 = 1,$$

$$g_3 = \bar{f}ig_4 = \bar{f}ig_5 = -g_6 = (1 + i e^{-sf_0(v)})^{-1},$$

$$\alpha c_0 f_0 = \frac{4}{3} \zeta^{3/2}(0),$$

$$\alpha c_0 f_1 = \alpha c_0 (f_5 - f_0) = \nu c_0 \alpha x + \frac{2}{3} \zeta^{3/2}(z) - \frac{2}{3} \zeta^{3/2}(z_1),$$

$$\alpha c_0 f_2 = \alpha c_0 (f_6 - f_0) = \nu c_0 \alpha x + \frac{2}{3} \zeta^{3/2}(z) + \frac{2}{3} \zeta^{3/2}(z_1),$$

$$\alpha c_0 f_3 = \nu c_0 \alpha x - \frac{2}{3} \zeta^{3/2}(z) - \frac{2}{3} \zeta^{3/2}(z_1) + \frac{4}{3} \zeta^{3/2}(0),$$

$$\alpha c_0 f_4 = \nu c_0 \alpha x - \frac{2}{3} \zeta^{3/2}(z) + \frac{2}{3} \zeta^{3/2}(z_1) + \frac{4}{3} \zeta^{3/2}(0),$$

while the upper signs are valid in $\text{Im } \nu s > 0$, the lower in $\text{Im } \nu s < 0$.

The expansions on the remainder of the path of integration are given in appendix 5. When we put $\tilde{U}_j = \int_L U_j^* dv$, where L denotes that part of $(-i\infty e^{-i\phi}, i\infty e^{-i\phi})$ on which U_j^* appears, the result of the inverse transformation is

$$(4.2) \quad \tilde{U} \sim \sum_{j=1}^6 \tilde{U}_j.$$

In the area of the x, z -plane where the j th integral has a saddle point its contribution can be evaluated by standard methods, in the complementary region its contribution is asymptotically of lower order and therefore it will not be taken into account (see again appendix 5). The only exception is $j = 3$. In this case the poles can be important.

Table 1 classifies the extremes of $f_j(\nu)$ ($j=1,2,\dots,6$) as functions of real positive ν and indicates the regions in the x, z -plane where the extremes occur. The numbers in the last column correspond to the numbers in figure 2. These regions are mapped in figure 3. In the following the saddle point of $f_j(\nu)$ will be denoted by ν_{sj} for all j except $j = 5$. In the latter case we use $\nu_{5\min}$ and $\nu_{5\max}$. The zero of $f_5''(\nu)$ will be denoted by ν_{c5} .

Several features stand out. The maximum of f_1 , resp. f_3 or f_5 , and the minimum of f_2 , resp. f_4 or f_6 , exist in complementary regions. As (x, z) tends to the boundary curve between two such regions ν tends to $\nu(z_1)$. The use of the exponential expansion for $H_N^{(1,2)sj}(\text{Nw}_1)$

Table 1

j	$\alpha f_j^i(\nu)$	Region	Type of extremum	
1	$\alpha x - [(1-w^2)^{\frac{1}{2}} - (1-w_1^2)^{\frac{1}{2}}] / \nu c_0$	$0 < \alpha x < [(1+\alpha z_1)^2 - (1+\alpha z)^2]^{\frac{1}{2}}$	maximum	I
1,2	$\alpha x - (1-w^2)^{\frac{1}{2}} / \nu c_0$	$\alpha x \leq [(1+\alpha z_1)^2 - (1+\alpha z)^2]^{\frac{1}{2}}$	minimum	III
2	$\alpha x - [(1-w^2)^{\frac{1}{2}} + (1-w_1^2)^{\frac{1}{2}}] / \nu c_0$	$\alpha x > [(1+\alpha z_1)^2 - (1+\alpha z)^2]^{\frac{1}{2}}$	minimum	II
3	$\alpha x + [(1-w^2)^{\frac{1}{2}} + (1-w_1^2)^{\frac{1}{2}} - 2(1-w_0^2)^{\frac{1}{2}}] / \nu c_0$	$0 < \alpha x < [(1+\alpha z_1)^2 - (1+\alpha z)^2]^{\frac{1}{2}} + 2[(1+\alpha z_1)^2 - 1]^{\frac{1}{2}}$	maximum	I
3,4	$\alpha x + [(1-w^2)^{\frac{1}{2}} - 2(1-w_0^2)^{\frac{1}{2}}] / \nu c_0$	$\alpha x \leq [(1+\alpha z_1)^2 - (1+\alpha z)^2]^{\frac{1}{2}} + 2[(1+\alpha z_1)^2 - 1]^{\frac{1}{2}}$	coincidence of two extremes if $(1+\alpha z) > \frac{1}{2}[3(1+\alpha z_1)^2 + 1]^{\frac{1}{2}}$ minimum if $(1+\alpha z) < \frac{1}{2}[3(1+\alpha z_1)^2 + 1]^{\frac{1}{2}}$	IV III
4	$\alpha x + [(1-w^2)^{\frac{1}{2}} - (1-w_1^2)^{\frac{1}{2}} - 2(1-w_0^2)^{\frac{1}{2}}] / \nu c_0$	$\alpha x > [(1+\alpha z_1)^2 - (1+\alpha z)^2]^{\frac{1}{2}} + 2[(1+\alpha z_1)^2 - 1]^{\frac{1}{2}}$	minimum	II
5	$\alpha x - [(1-w^2)^{\frac{1}{2}} - (1-w_1^2)^{\frac{1}{2}} + 2(1-w_0^2)^{\frac{1}{2}}] / \nu c_0$	$\alpha x > \alpha[x - f_5^i(\nu_{c5})]$ $\alpha x \leq \alpha[x - f_5^i(\nu_{c5})]$	minimum	II
		$\alpha[x - f_5^i(\nu_{c5})] < \alpha x < [(1+\alpha z_1)^2 - (1+\alpha z)^2]^{\frac{1}{2}} + 2[(1+\alpha z_1)^2 - 1]^{\frac{1}{2}}$	coincidence of two extremes	V
5,6	$\alpha x - [(1-w^2)^{\frac{1}{2}} + 2(1-w_0^2)^{\frac{1}{2}}] / \nu c_0$	$\alpha x \leq [(1+\alpha z_1)^2 - (1+\alpha z)^2]^{\frac{1}{2}} + 2[(1+\alpha z_1)^2 - 1]^{\frac{1}{2}}$	maximum	I
6	$\alpha x - [(1-w^2)^{\frac{1}{2}} + (1-w_1^2)^{\frac{1}{2}} + 2(1-w_0^2)^{\frac{1}{2}}] / \nu c_0$	$\alpha x > [(1+\alpha z_1)^2 - (1+\alpha z)^2]^{\frac{1}{2}} + 2[(1+\alpha z_1)^2 - 1]^{\frac{1}{2}}$	minimum	II
		$\alpha x > [(1+\alpha z_1)^2 - (1+\alpha z)^2]^{\frac{1}{2}} + 2[(1+\alpha z_1)^2 - 1]^{\frac{1}{2}}$	minimum	II

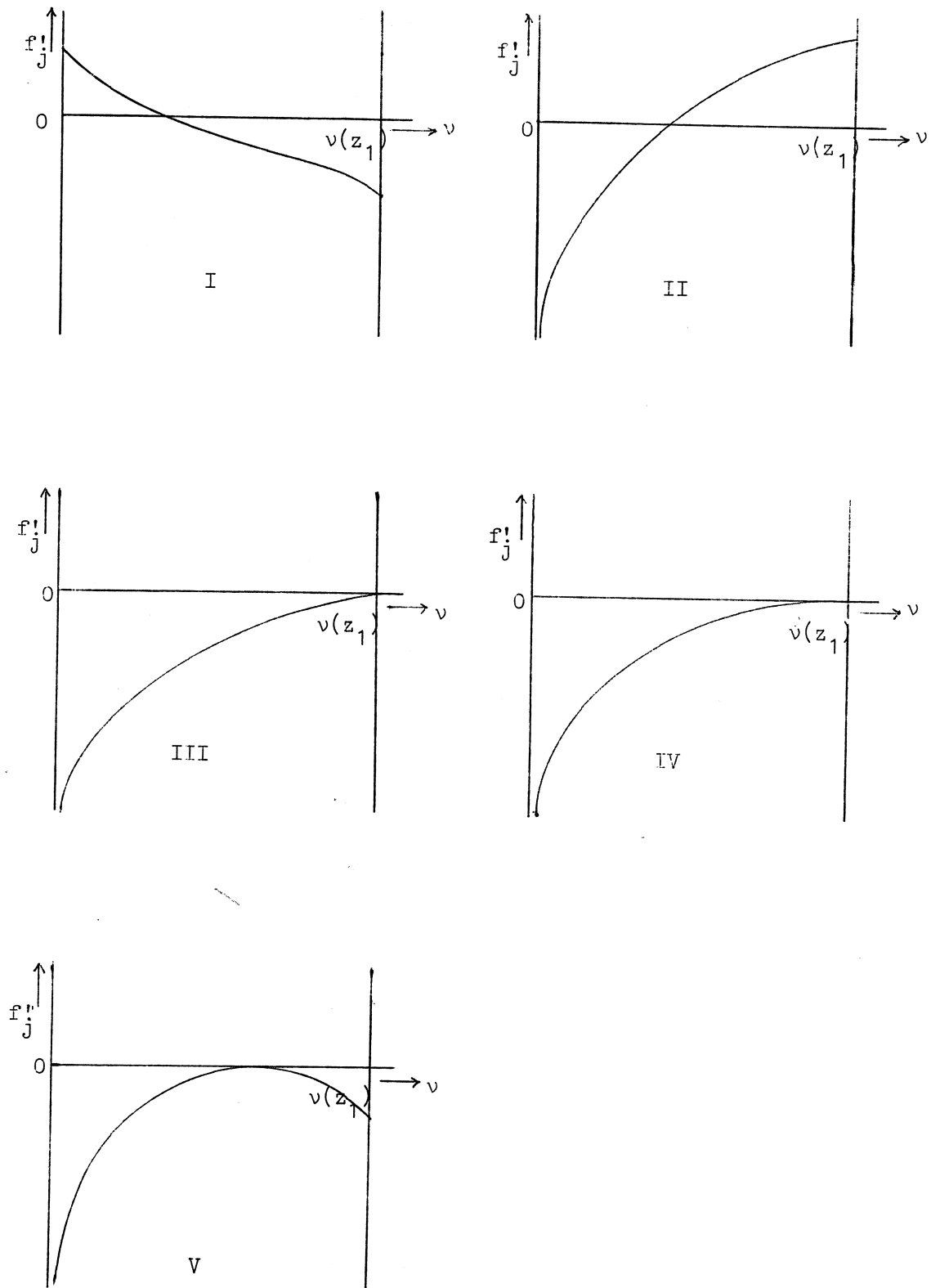


Figure 2. The behaviour of the first-order derivatives.

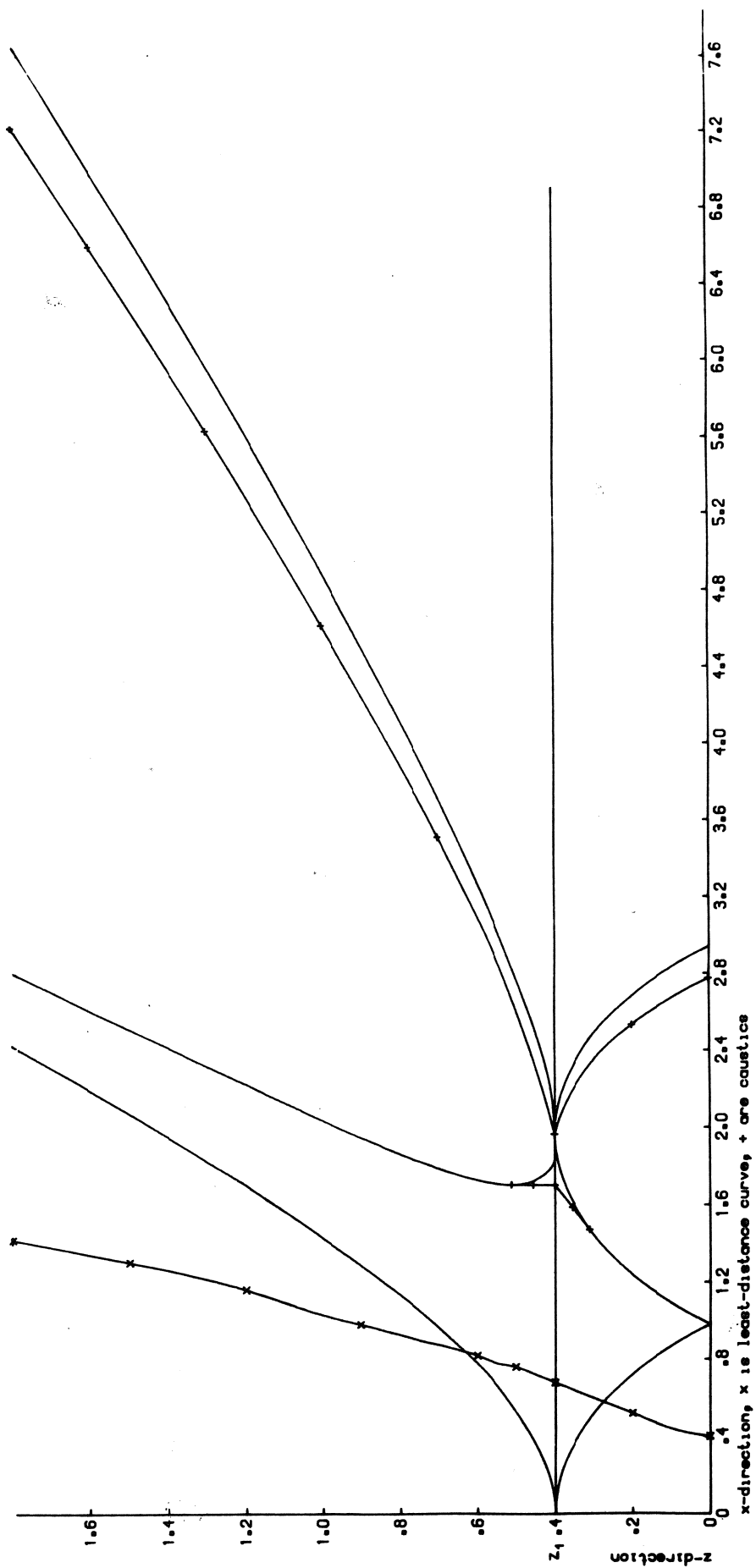


Figure 3. A map of the x, z -plane.

is then no longer permitted and the term connected with z_1 vanishes from the exponential part of U_j^* (see table 1, second column). When $0 \leq z \leq z_1$ the boundary curves correspond to the path of the ray which leaves the source parallel to the positive x -axis and when $z \geq z_1$ the boundary curves are the loci of the turning points of the rays, i.e. regions where ray theory no longer holds.

There are a numbers of caustics, i.e. curves on which $f_j' = f_j'' = 0$ holds. We only find two of them (see figure 3) because the factor $(1+i \exp -sf_0)^{-1}$ has not been expanded completely. Viz.

$$\alpha x = 3^{1/2} [(1+\alpha z)^2 - 1]^{1/2} \text{ for } \frac{1}{2} [3(1+\alpha z_1)^2 + 1]^{1/2} \leq (1+\alpha z) \leq (1+\alpha z_1)$$

in connection with f_{34} and $f_5'(v_{c5}) = 0$ in connection with f_5 . As f_{34} is only needed close to $\alpha x = -[(1+\alpha z_1)^2 - (1+\alpha z)^2]^{1/2} + 2[(1+\alpha z_1)^2 - 1]^{1/2}$ only part of the first-mentioned curve will behave like a caustic depending on the proximity of the two curves.

Details of the evaluation of the saddle-point contributions can be found in appendix 5. Here we only state the results. Writing

$$(4.3) \quad F = \int_L g(v) e^{-sf(v)} dv,$$

$$\text{we get} \quad F \sim \left(\frac{2\pi}{s|f''(v_s)|} \right)^{1/2} g(v_s) e^{-sf(v_s) + \pi i/2}, \text{ if } v = v_s \text{ is a maximum,}$$

$$\sim \pm \left(\frac{2\pi}{sf''(v_s)} \right)^{1/2} g(v_s) e^{-sf(v_s)}, \text{ if } v = v_s \text{ is a minimum,}$$

$$\sim \frac{2\pi}{3^{2/3}\Gamma(2/3)} \left(\frac{2}{s|f'''(v_c)|} \right)^{1/3} g(v_c) e^{-sf(v_c) + \pi i/6},$$

$$\text{if } v = v_c \text{ is a caustic.}$$

Using the above formulae we find inside the regions of validity indicated in table 1 and figure 3.

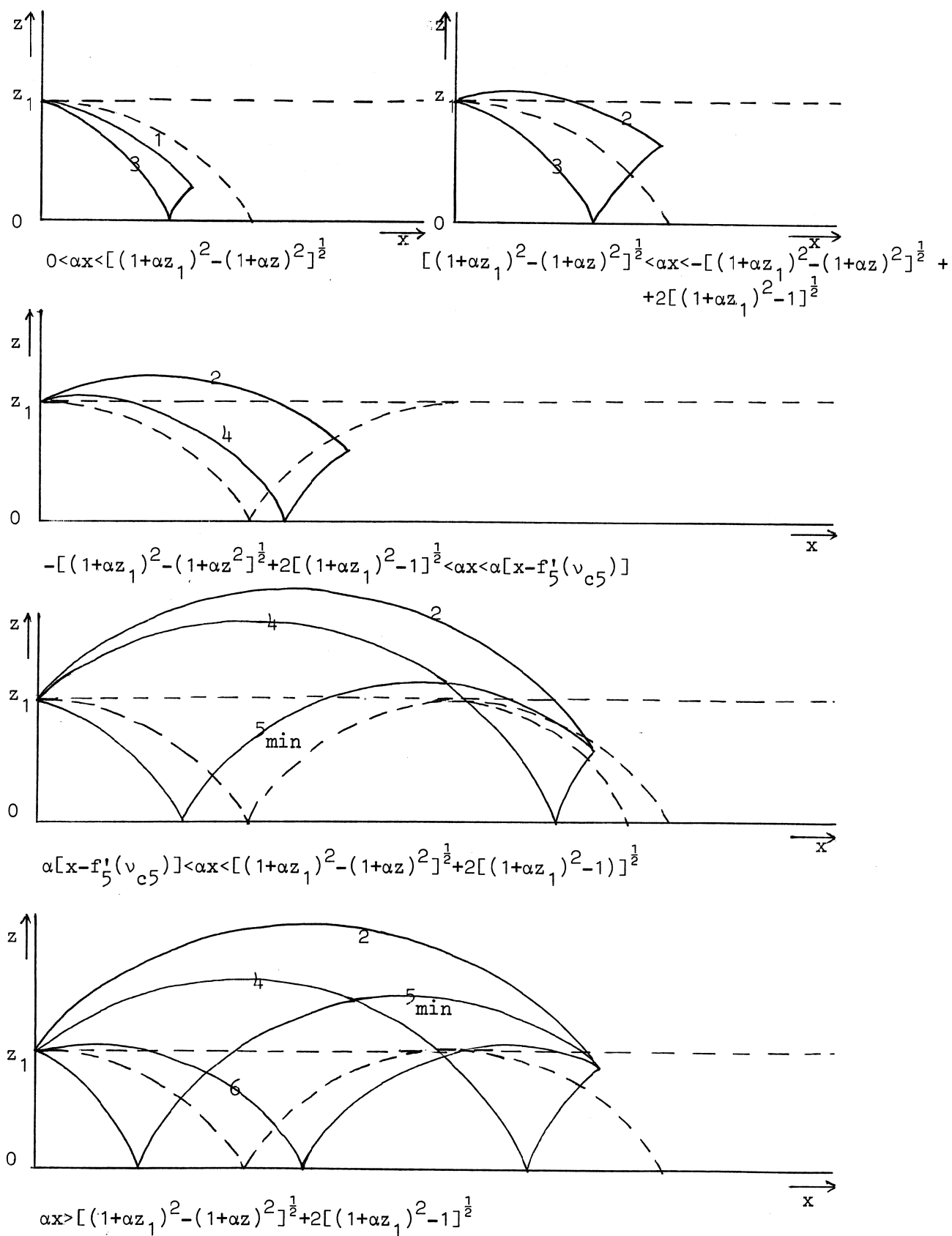


Figure 4. The rays in different regions of the x, z -plane, $0 < z < z_1$.

$$\begin{aligned}
(4.4) \quad \tilde{U}_j &\sim \frac{c_0(1+\alpha z_1)}{2^{3/2} \pi^{1/2}} \chi s^{-1/2} \{ (1-w_1^2)^{-1/4} (1-w^2)^{-1/4} |f_j''|^{-1/2} \}_{v=v_{sj}} \cdot \\
&\cdot e^{-s\tau_j} [1+O(s^{-1/2})], \quad j = 1, 2, 3, 4, 5 \text{ min}, \\
&\sim \frac{c_0(1+\alpha z_1)}{2^{3/2} \pi^{1/2}} \chi s^{-1/2} \{ (1-w_1^2)^{-1/4} (1-w^2)^{-1/4} |f_j''|^{-1/2} \}_{v=v_{sj}} \cdot \\
&\cdot e^{-s\tau_j \pm \pi i/2} [1+O(s^{-1/2})], \quad j = 5 \text{ max}, 6,
\end{aligned}$$

where $\tau_j = f_j(v_{sj})$ is the arrival time of the corresponding ray (figure 4),

$(1+i \exp-sf_0)^{-1}$ is approximated by 1

and the upper signs hold for $\text{Im } s > 0$.

Near the boundary curves but away from the caustics

$$\begin{aligned}
(4.5) \quad \tilde{U}_j + \tilde{U}_{j+1} &\sim \pm \frac{c_0(1+\alpha z_1)}{6^{2/3} \Gamma(2/3)} \chi \left(\frac{\alpha c_0}{s}\right)^{1/3} (\alpha c_0)^{-1/2} \{ (1-w^2)^{-1/4} \cdot \\
&\cdot |f_{j,j+1}''|^{-1/2} \}_{v=v_{j,j+1}} e^{-s\tau_{j,j+1} \mp \pi i/3} [1+O(s^{-1/3})],
\end{aligned}$$

where $j = 1, 3, 5 \text{ max}$,

$$\alpha c_0 \tau_{12} = v c_0 \alpha x + \frac{2}{3} \zeta_{(z)}^{3/2} \quad \text{with } v c_0 = v_{12} c_0 = [(\alpha x)^2 + (1+\alpha z)^2]^{1/2},$$

$$\alpha c_0 \tau_{34} = v c_0 \alpha x - \frac{2}{3} \zeta_{(z)}^{3/2} + \frac{4}{3} \zeta_{(0)}^{3/2} \quad \text{with } v = v_{34} \text{ following from}$$

$$v c_0 \alpha x = 2(1-w_0^2)^{1/2} - (1-w^2)^{1/2},$$

$$\text{and } \alpha c_0 \tau_{56} = v c_0 \alpha x + \frac{2}{3} \zeta_{(z)}^{3/2} + \frac{4}{3} \zeta_{(0)}^{3/2} \quad \text{with } v = v_{56} \text{ following from}$$

$$v c_0 \alpha x = 2(1-w_0^2)^{1/2} + (1-w^2)^{1/2}.$$

Near the caustics

$$(4.6) \quad \tilde{u}_3 + \tilde{u}_4 \sim \frac{2^{5/6} \pi^{1/2} (1+\alpha z_1)}{3^{7/6} \Gamma(2/3)} \chi\left(\frac{\alpha c_0}{s}\right)^{1/3} [(1+\alpha z)^2 - 1]^{1/4} \cdot \\ \cdot [4(1+\alpha z)^2 - 1]^{-3/4} e^{-s\tau_{c34} \pm \pi i/6 - \pi i/2} [1+O(s^{-1/3})],$$

with $\tau_{c34} = \tau_{34}$ where $\nu c_0 = \nu_{c34} c_0 = 3^{1/2} [4(1+\alpha z)^2 - 1]^{-1/2}$ and

$$(4.7) \quad \tilde{u}_{5\max} + \tilde{u}_{5\min} \sim \frac{c_0 (1+\alpha z_1)}{6^{2/3} \Gamma(2/3)} \chi\left(\frac{\alpha c_0}{s}\right)^{1/3} \{(1-w_1^2)^{-1/4} (1-w^2)^{-1/4} \cdot \\ \cdot (\alpha c_0 |f_5''')^{-1/3}\}_{\nu=\nu_{c5}} e^{-s\tau_{c5} \pm \pi i/6} [1+O(s^{-1/3})],$$

with $\tau_{c5} = f_5(\nu_{c5})$ and $\nu = \nu_{c5}$ obtained numerically from $f_5'' = 0$.

When we deform the original line of integration into the steepest-descent path for $j = 3$ it is possible that a number of poles are passed. The path of the steepest descent is given by $\text{Im}\{e^{i\phi} f_3(\nu)\} = \text{Im}\{e^{i\phi} f_3(\nu_{s3})\}$. A sufficient indication of the location of the poles with respect to this curve is obtained by checking whether the curve recrosses the positive real ν -axis at any point. Considered as a function of ϕ $\text{Im}\{e^{i\phi} f_3(\nu)\}$ takes its maximum values for real positive ν when $\phi = \pi/2$, so that, if the steepest-descent path recrosses this axis for any value of ϕ it will certainly do so when $\phi = \pi/2$. Therefore we may confine ourselves to studying the behaviour of $\text{Im}\{e^{i\pi/2} f_3(\nu)\} = \text{Re}\{f_3(\nu)\} = f_3(\nu_{s3})$. The function $\text{Re}\{f_3(\nu)\}$ shows one maximum for $0 \leq \nu \leq \nu(z_1)$, either one minimum or two minima and one maximum for $\nu(z_1) < \nu < \nu(0)$ and increases steadily afterwards. This implies that the poles must be taken into account when $\text{Re}\{f_3(\nu(0))\} = x/c_0 \geq f_3(\nu_{s3})$ and this is the "least-distance" criterium we wanted to obtain. The curve $x/c_0 = f_3(\nu_{s3})$ has been computed numerically and is plotted in figure 3. The influence of the normal modes becomes noticeable to the right of this curve.

5. The inverse Laplace transform.

Using the contour integral method we obtained in (3.6)

$$\tilde{U} = \frac{\pi i}{2} c_0 (1 + \alpha z_1) \chi \frac{s}{\alpha c_0} \sum_{k=1}^K \tilde{R}_k,$$

where $i\tilde{R}_k$ takes complex conjugate values at complex conjugate points of the s -plane. It follows that

$$(5.1) \quad U = \frac{1}{4} \frac{(1 + \alpha z_1)}{\alpha} \chi \int_{s_0 - i\infty}^{s_0 + i\infty} s e^{st} \sum_{k=1}^K \tilde{R}_k ds,$$

where s_0 is large and K depends on s and ϕ .

When we consider \tilde{R}_k as a function of s in $\text{Im } s > 0$ we find that

$$\tilde{R}_k = 0 \text{ of } s \in (s_0, s_0 + i\delta_k),$$

while for fixed k and $s_0 \rightarrow \infty$ $\delta_k \rightarrow 0$. This implies that we may use the \tilde{R}_k -approximation for small $\zeta_k(0)$ almost everywhere. Only when ϕ approaches $\pi/2$ (and $\delta_k \rightarrow \infty$) the approximation for large $\zeta_k(0)$ must be used. The separate terms of \tilde{U} are Laplace transforms because they show the correct behaviour at infinity, i.e.

$$(5.2) \quad \begin{aligned} & |s e^{x/c_0} \tilde{R}_k| \rightarrow 0 && \text{for small } \zeta_k(0), \\ & |(s/\alpha c_0) \ln(1 + \alpha z_1)(1 + \alpha z) \tilde{R}_k| \rightarrow 0 && \text{for large } \zeta_k(0), \end{aligned}$$

when $|s| \rightarrow \infty$ in $0 < \phi < \pi/2$.

For $s_0 \rightarrow \infty$ both $\delta_k \rightarrow 0$ and $K \rightarrow \infty$, therefore

$$(5.3) \quad U = \sum_{k=1}^{\infty} R_k \text{ with}$$

$$(5.4) \quad R_k = \frac{1}{4} \frac{(1 + \alpha z_1)}{\alpha} \chi \int_{s_0 - i\infty}^{s_0 + i\infty} s e^{st} \tilde{R}_k ds,$$

where \tilde{R}_k is known on all of the path of integration except for an arbitrarily small section surrounding $\text{Im } s = 0$.

In the following $\bar{\tau}_0$ denotes the complex conjugate of τ_0 etc. We move the contour to the imaginary axis. This is allowed for the \tilde{R}_k are well behaved functions, but we must keep in mind that the approximations were valid for large $\text{Re } s$ and that consequently the results will be valid for small $(t - \text{Re } \tau_0)$ only.

The origin is excluded by a small half circle in $\text{Re } s > 0$. It is easy to prove that the contribution of this half circle tends to zero with its radius even though \tilde{R}_k is not completely known. We substitute $s = i\sigma^3$ when $\text{Im } s > 0$ and $s = -i\sigma^3$ when $\text{Im } s < 0$.

$$\begin{aligned} R_k &= - \frac{3.2^{-7/3}}{\pi^2} (1 + \alpha z_1) \chi(\alpha c_0)^{2/3} \epsilon_0 \text{Re} \left\{ \int_0^\infty \exp i[\sigma^3(t - \tau_0) + \right. \\ &\quad \left. + (2\alpha c_0)^{-1/3} (-a'_k) \delta_0^\sigma] d\sigma \right\} \\ &= - C(x, z) \text{Re} \left\{ \int_0^\infty \exp(-\sigma^3[\tau_0^* - i(t - \frac{x}{c_0})] + i\sigma(2\alpha c_0)^{-1/3} (-a'_k) \delta_0) d\sigma \right\}, \end{aligned}$$

where the meaning of $C(x, z)$ is obvious and $\tau_0^* = i(\tau_0 - x/c_0)$.

In the above $(t - x/c_0)$ is very small so that we may use $\lambda = (t - x/c_0)^{-1}$ as a large parameter. We introduce a new variable κ by $\kappa = \sigma(t - x/c_0)^{1/3}$ and obtain

$$R_k = - C(x, z) \lambda^{1/3} \text{Re} \left\{ \int_0^\infty \exp[-\kappa^3(\lambda \tau_0^* - i) + i\kappa \lambda^{1/3} (2\alpha c_0)^{-1/3} (-a'_k) \delta_0] d\kappa \right\}.$$

This integral converges in the complex κ -plane when $|\kappa| \rightarrow \infty$ in one of three sectors, viz.

$$\begin{aligned} & - \pi/6 + \frac{1}{3} \text{arctg}(\lambda \tau_0^*)^{-1} + 2n\pi/3 < \arg \kappa < \\ & < \pi/6 + \frac{1}{3} \text{arctg}(\lambda \tau_0^*)^{-1} + 2n\pi/3, \quad n = 0, 1, 2. \end{aligned}$$

The saddle points of the integrand follow from

$$-3\kappa^2(\lambda\tau_0^*-i) + i(\lambda/2\alpha c_0)^{1/3}(-a_k')\delta_0 = 0 \text{ as}$$

$$\kappa = \pm \kappa_s = \pm \left| \frac{i(\lambda/2\alpha c_0)^{1/3}(-a_k')\delta_0}{3(\lambda\tau_0^*-i)} \right|^{1/2},$$

where $0 < \arg \kappa_s < \pi/4$ and $|\kappa_s|$ is very small.

The original path of integration may be deformed to pass through $\kappa = \kappa_s$ and tend to infinity inside the sector $n = 0$. The direction of the path of steepest descent in $\kappa = \kappa_s$ follows from

$$\kappa_s(\lambda\tau_0^*-i)(\kappa-\kappa_s)^2 \text{ positive and real as}$$

$$\arg(\kappa-\kappa_s) = -\frac{1}{2} \arg \kappa_s - \frac{1}{2} \arg(\lambda\tau_0^*-i)^{-1}.$$

It follows that

$$(5.5) \quad R_k \sim -\left(\frac{3\alpha c_0}{8\pi^2}\right)^{3/4} (1+\alpha z_1) \chi \epsilon_0 (-a_k')^{-1/4} \cdot \frac{\exp\left[-\frac{1}{3}\left(\frac{2}{3\alpha c_0}\right)^{1/2}(-a_k')^{3/2}\delta_0^{3/2}(t-\tau_0)^{-1/2}\right]}{\delta_0^{1/4}(t-\tau_0)^{1/4}} \cdot \text{Re}\{ \dots \} H(t-x/c_0).$$

Using the saddle point method we obtained the results (4.4), (4.5), (4.6) and (4.7). We put $U_j = \frac{1}{2\pi i} \int_{s_0-i\infty}^{s_0+i\infty} e^{st} \tilde{U}_j ds$, where again \tilde{U}_j is known explicitly on all of $(s_0-i\infty, s_0+i\infty)$ except for a small section surrounding $s = s_0$. Again we can move the contour to the imaginary axis avoiding $s = 0$ with a semi-circle in $\text{Re } s > 0$ with vanishing radius which doesn't contribute. Then we find

$$(5.6) \quad U_j \sim \frac{c_0(1+\alpha z_1)}{2^{3/2}\pi} \chi\{(1-w_1^2)^{-1/4}(1-w^2)^{-1/4} |f_j''|^{-1/2}\}_{v=v_{sj}} \cdot \frac{H(t-\tau_j)}{(t-\tau_j)^{1/2}} [1+O((t-\tau_j)^{1/2})], \quad j = 1, 2, 3, 4, 5 \text{ min.}$$

If $j = 5$ max or 6 the contribution of the first term of the asymptotic expansion is zero. Therefore the displacement for $t \sim \tau_j$ will be at most of order $O(1)$, that is small compared to the preceding displacements.

Near the boundary curves for $j = 1, 3, 5$ max,

$$(5.7) \quad U_j + U_{j+1} \sim \frac{c_0(1+\alpha z_1)}{2^{2/3}(3\alpha c_0)^{1/6}} \chi\{(1-w^2)^{-1/4} |f''_{j,j+1}|^{-1/2}\}_{v=v_{j,j+1}} \cdot \\ \cdot \frac{H(t-\tau_{j,j+1})}{(t-\tau_{j,j+1})^{2/3}} [1+O((t-\tau_{j,j+1})^{1/3})].$$

Near the caustics

$$(5.8) \quad U_3 + U_4 \sim \frac{(\alpha c_0)^{1/3} (1+\alpha z_1)}{2^{1/6} 3^{7/6} \pi^{1/2} \Gamma(2/3)} \chi[(1+\alpha z)^2 - 1]^{1/4} [4(1+\alpha z)^2 + 1]^{-3/4} \cdot \\ \cdot e^{-\pi i/3} \frac{H(t-\tau_{c34})}{(t-\tau_{c34})^{2/3}} [1+O((t-\tau_{c34})^{1/3})]$$

and

$$(5.9) \quad U_{5\max} + U_{5\min} \sim \frac{c_0(1+\alpha z_1)}{2^{5/3} 3^{1/6} \pi} \chi\{(1-w_1^2)^{-1/4} (1-w^2)^{-1/4} |f'''_5|^{-1/3}\}_{v=v_{c5}} \cdot \\ \cdot e^{\pi i/6} \frac{H(t-\tau_{c5})}{(t-\tau_{c5})^{2/3}} [1+O((t-\tau_{c5})^{1/3})].$$

It is of course possible to refine the results obtained in sections 3, 4 and 5 by taking higher order terms of the asymptotic expansions, but this is neither very attractive nor useful as the important features of the problem have already come to light in the foregoing.

References

- [1] Abramowitz, M., and I.A. Stegun, Handbook of mathematical functions, N.B.S. Appl. Math. Ser. 55, Washington D.C. (1965).
- [2] Babich, V.M., and A.S. Alekseev, A ray method of computing wave front intensities, Izv. Geophys. Ser. (1958), 17-31.
- [3] Brekhovskikh, L.M., Waves in layered media, Academic Press, New York - London (1960).
- [4] de Bruyn, N.G., Asymptotic methods in analysis, North-Holland Publishing Co., Amsterdam - P. Noordhoff Ltd., Groningen (1958).
- [5] Grimshaw, R., The refraction of sound pulses, Proc. Camb. Phil. Soc. 63 (1967), 1247-1272.
- [6] Keller, J.B., A geometrical theory of diffraction, Proc. Symp. Appl. Math. VIII (1958), 27-52.
- [7] Lapwood, E.R., The disturbance due to a line source in a semi-infinite elastic medium, Phil. Trans. Roy. Soc. (London) A242 (1949), 63-100.
- [8] Maulik, T.N., On the effect of low-velocity channel inside the earth, Bull. Seism. Soc. Am. 55 (1965), 121.
- [9] Newlands, M., On a line source in an elastic medium with a single surface layer, Phil. Trans. Roy. Soc. London) A245 (1952), 213-308.
- [10] Olver, F.W.J., The asymptotic expansion of Bessel functions of large order, Phil. Trans. Roy. Soc. (London) A247 (1954), 328-368.

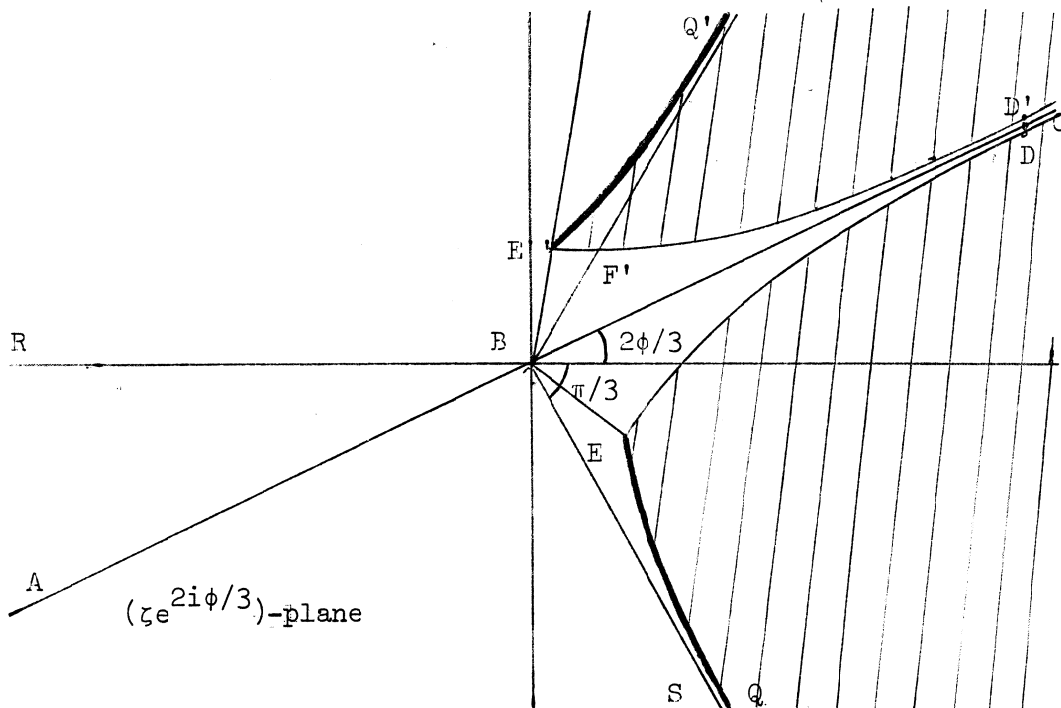
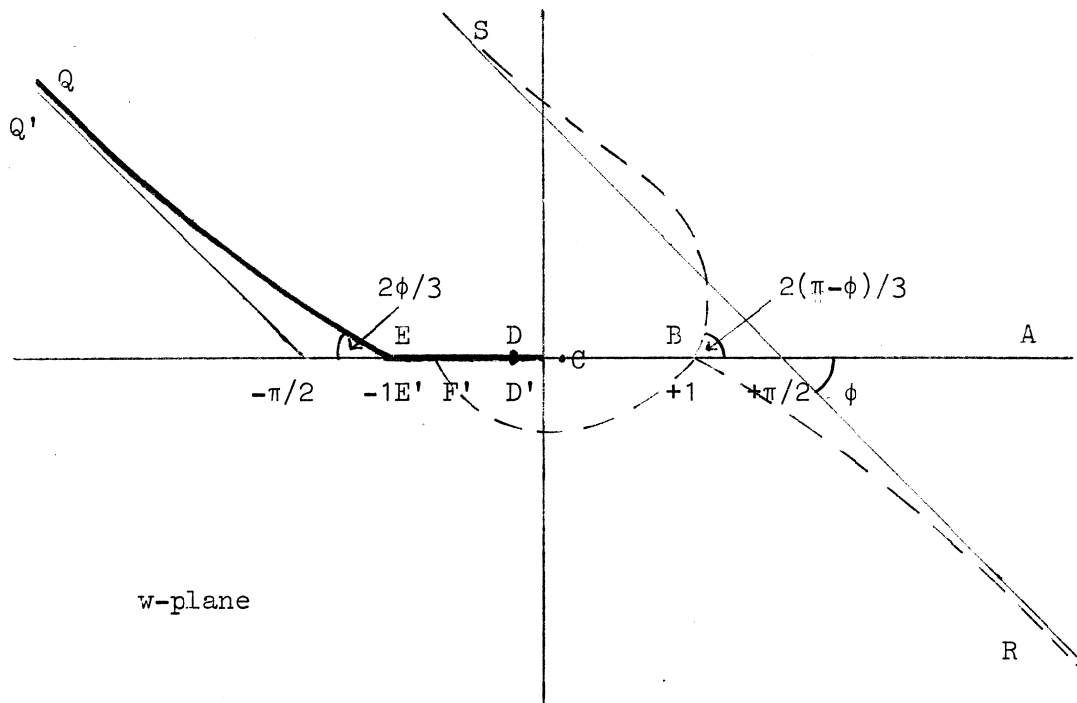


Figure 5. The mapping $\frac{2}{3} \zeta^{3/2} = \int_w^1 \frac{(1-\beta^2)^{1/2}}{\beta} d\beta$.

Appendix 1. Uniform asymptotic expansion of Bessel functions.

Details of the uniform asymptotic expansions for Bessel functions of large order and large argument can be found in Olver's paper [10]. Some of the formulae have been taken from the Handbook of Mathematical Functions [1].

We only repeat as an example

$$H_N^{(1)}(Nw) \sim 2^{3/2} e^{-\pi i/3} N^{-1/3} \left(\frac{\zeta}{1-w^2} \right)^{1/4} \{ \text{Ai}(e^{2\pi i/3} N^{2/3} \zeta) \sum_{m=0}^{\infty} A_m(\zeta) N^{-2m} + \\ + e^{2\pi i/3} N^{-4/3} \text{Ai}'(e^{2\pi i/3} N^{2/3} \zeta) \sum_{m=0}^{\infty} B_m(\zeta) N^{-2m} \},$$

where ζ is real when w is real and positive,

$$\frac{2}{3} \zeta^{3/2} = \int_w^1 \frac{(1-\beta^2)^{1/2}}{\beta} d\beta = - (1-w^2)^{1/2} + \ln \frac{1+(1-w^2)^{1/2}}{w}$$

(the mapping of the w -plane on the ζ -plane is shown in figure 5),

$$A_0(\zeta) = 1$$

and the other coefficients $A_m(\zeta)$, $B_0(\zeta)$, $B_m(\zeta)$ ($m=1,2,\dots$) follow from a set of recursive relations.

$H_N^{(2)}(Nw)$ follows from the above by changing all factors i to $-i$, while $J_N(Nw) = \frac{1}{2} [H_N^{(1)}(Nw) + H_N^{(2)}(Nw)]$.

Everywhere in $\text{Re}(w e^{i\phi}) \geq 0$ except very near $w = 1$ we can replace the Airy functions by their exponential asymptotic expansions, e.g.

$$H_N^{(1)}(Nw) \sim (2/\pi N)^{1/2} (1-w^2)^{-1/4} \exp\left(\frac{2}{3} N \zeta^{3/2} - \frac{\pi i}{2}\right), \quad -\pi \leq \arg N^{2/3} \zeta \leq -\pi/3, \\ \sim (2/N)^{1/2} (1-w^2)^{-1/4} \left[\exp\left(-\frac{2}{3} N \zeta^{3/2}\right) + \exp\left(\frac{2}{3} N \zeta^{3/2} - \frac{\pi i}{2}\right) \right],$$

$$-\pi/3 < \arg N^{2/3} \zeta < \pi.$$

Appendix 2. Poles of the solution for small $\zeta(0)$.

Near $v = v(0)$ we may put

$$\zeta(0) = 2^{-2/3}(1-w_0^2) \{1 + \frac{2}{5}(1-w_0^2) + o((1-w_0^2)^2)\}.$$

We suppose that $N^{2/3}\zeta(0)$ is finite and try the expansion

$$N^{2/3}\zeta(0) = \beta + \gamma(2/N)^{1/3} + o(N^{-2/3}),$$

which implies $1 - w_0^2 = \beta(2/N)^{2/3} + \gamma(2/N) + o(N^{-4/3})$.

Also
$$\left(\frac{1-w_0^2}{\zeta(0)}\right)^{\pm 1/4} = 2^{\pm 1/6} [1 + o(N^{-2/3})],$$

$$\text{Ai}(e^{2\pi i/3} N^{2/3} \zeta(0)) = \text{Ai}(e^{2\pi i/3} \beta) + e^{2\pi i/3} \gamma \text{Ai}'(e^{2\pi i/3} \beta) (2/N)^{1/3} + o(N^{-2/3}),$$

and

$$\begin{aligned} \text{Ai}'(e^{2\pi i/3} N^{2/3} \zeta(0)) &= \text{Ai}'(e^{2\pi i/3} \beta) + e^{4\pi i/3} \beta \gamma \text{Ai}(e^{2\pi i/3} \beta) (2/N)^{1/3} + \\ &\quad + o(N^{-2/3}). \end{aligned}$$

With these approximations in $0 < \phi < \pi/2$

$$\begin{aligned} W^- &= -2^{5/3} e^{\pi i/3} N^{1/3} [1 + o(N^{-2/3})] \{ \text{Ai}'(e^{2\pi i/3} \beta) + \\ &\quad + e^{4\pi i/3} \beta \gamma \text{Ai}(e^{2\pi i/3} \beta) (2/N)^{1/3} + \\ &\quad + N^{-2/3} [2^{-1/6} e^{\pi i/3} \text{Ai}(e^{2\pi i/3} \beta) + o(1) + o(N^{-2/3})] \}, \end{aligned}$$

i.e. $W^- = 0$, if $\beta = \beta_k = e^{-2\pi i/3} a'_k$ ($k=1,2,\dots$) and $\gamma = 0$, where a'_k is the k th zero of $\text{Ai}'(z)$ and is real and negative.

It follows that $N^{2/3}\zeta_k(0) = e^{-2\pi i/3} a'_k + o(N^{-2/3})$

and
$$1 - w_{0k}^2 = e^{-2\pi i/3} a'_k (2/N)^{2/3} + o(N^{-4/3}).$$

Appendix 3. Calculation of the residues for small $\zeta(0)$.

Again we take $0 < \phi < \pi/2$ as an example. We want to compute

$$\tilde{R}_k = \left[\frac{W^+}{(\partial W^- / \partial v)} e^{-vsx} H_N^{(1)}(Nw) H_N^{(1)}(Nw_1) \right]_{v=v_k}.$$

Now

$$\begin{aligned} \left. \frac{\partial W^-}{\partial v} \right|_{v=v_k} &= \frac{\partial W^-}{\partial w_0} \left. \frac{\partial w_0}{\partial v} \right|_{v=v_k} \\ &= \frac{c_0}{w_{0k}} \left[(1-w_0^2) N^2 H_N^{(1)}(Nw_0) + \frac{1-p}{2} N w_0 H_N^{(1)'}(Nw_0) \right]_{w_0=w_{0k}}. \end{aligned}$$

and

$$w_{0k} = 1 - 2^{-1/3} e^{\pi i/3} (-a'_k) \left(\frac{\alpha c_0}{s} \right)^{2/3} + o(s^{-4/3}).$$

We find

$$\left. \frac{\partial W^-}{\partial v} \right|_{v=v_k} = 4c_0 (-a'_k) \text{Ai}(a'_k) \left(\frac{s}{\alpha c_0} \right) [1 + o(s^{-2/3})],$$

$$W^+ \Big|_{v=v_k} = \frac{2^{-1/3}}{\pi} \frac{e^{-\pi i/6}}{\text{Ai}(a'_k)} \left(\frac{ss}{\alpha c_0} \right)^{1/3} [1 + o(s^{-2/3})]$$

and

$$e^{-vsx} H_N^{(1)}(Nw) H_N^{(1)}(Nw_1) =$$

$$- \frac{2}{\pi} \left(\frac{\alpha c_0}{s} \right) [(1+\alpha z_1)^2 - 1]^{-1/4} [(1+\alpha z)^2 - 1]^{-1/4}.$$

$$\cdot \exp[-s\tau_0 + 2^{-1/3} e^{\pi i/3} (-a'_k) \delta_0 \left(\frac{s}{\alpha c_0} \right)^{1/3} + \frac{\pi i}{2}] [1 + o(s^{-1/3})],$$

where

$$\alpha c_0 \tau_0 = qx - i \left[\int_1^{(1+\alpha z_1)} + \int_1^{(1+\alpha z)} \right] \frac{(w^2 - 1)^{1/2}}{w} dw$$

and $\delta_0 = \alpha x - i [(1+\alpha z_1)^2 - 1]^{1/2} - i [(1+\alpha z)^2 - 1]^{1/2}.$

Combining these results we find

$$\tilde{R}_k = \frac{2^{-4/3}}{\pi^2 c_0} \left(\frac{\alpha c_0}{s}\right)^{5/3} \epsilon_0 \exp[-s\tau_0 + 2^{-1/3} e^{\pi i/3} \delta_0 \left(\frac{s}{\alpha c_0}\right)^{1/3} - \frac{2\pi i}{3}].$$

$$. [1 + O(s^{-1/3})],$$

where

$$\epsilon_0 = \frac{[(1+\alpha z_1)^2 - 1]^{-1/4} [(1+\alpha z)^2 - 1]^{-1/4}}{(-a_k^{\dagger}) \text{Ai}^2(a_k^{\dagger})}.$$

Appendix 4. The geometrical part of the solution.

According to ray theory [2], [3], [6] we may use the expression

$$U^{(n)}(x, z, t) = (1+\alpha z)^{-p/2} (1+\alpha z_1)^{p/2} \sum_{k=0}^{\infty} u_k^{(n)}(x, z) f_k[t - \tau^{(n)}(x, z)]$$

near the wave front of the n -times reflected wave.

The $u_k^{(n)}$ are analytic functions of x and z and

$$f'_k(t) = f_{k-1}(t),$$

while $f_0(t) = (\pi t)^{-1/2} H(t)$ and $H(t)$ denotes Heaviside's stepfunction. The equation $t = \tau^{(n)}(x, z)$ is the equation of the wave front. The wave equation is satisfied by the above series if

$$\nabla \tau^{(n)} \cdot \nabla \tau^{(n)} = 1/c^2,$$

$$2(\nabla u_0^{(n)} \cdot \nabla \tau^{(n)}) + u_0^{(n)} \Delta \tau^{(n)} = 0$$

$$\text{and} \quad 2(\nabla u_{k+1}^{(n)} \cdot \nabla \tau^{(n)}) + u_{k+1}^{(n)} \Delta \tau^{(n)} = \Delta u_k^{(n)} - \frac{p(p-2)}{4} \frac{\alpha^2}{(1+\alpha z)^2} u_k^{(n)},$$

$$k = 0, 1, 2, \dots,$$

are satisfied.

The rays are determined by $\frac{dx}{d\sigma} = \frac{\partial \tau}{\partial x} = \lambda$ and $\frac{dz}{d\sigma} = \frac{\partial \tau}{\partial z} = \pm \left(\frac{1}{c^2} - \lambda^2\right)^{1/2}$,

where σ is a parameter along the ray. On a ray leaving the source at an angle θ_1 with the negative z -axis we have $\lambda = \sin \theta_1 / c_0(1+\alpha z_1)$, $0 \leq \theta_1 \leq \pi$ for $x \geq 0$, and it follows from Snell's law that the angle $\theta(z)$ between the ray and the negative z -axis at any point is given by

$$\frac{\sin \theta_1}{c_0(1+\alpha z_1)} = \frac{\sin \theta(z)}{c_0(1+\alpha z)}.$$

A ray has turning points for $z = z_t$ with $z_t = (1 - \sin\theta(0))/\alpha \sin\theta(0)$ and is determined by the equations

$$x = -\frac{1+\alpha z_1}{\alpha} \cotg \theta_1 + n\Delta x + \frac{1+\alpha z}{\alpha} \cotg \theta(z)$$

and
$$\tau = -\frac{1}{2\alpha c_0} \ln \frac{1+\cos\theta_1}{1-\cos\theta_1} + n\Delta\tau + \frac{1}{2\alpha c_0} \ln \frac{1+\cos\theta(z)}{1-\cos\theta(z)},$$

where
$$\Delta x = \frac{2}{\alpha} \cotg \theta(0),$$

$$\Delta\tau = \frac{1}{\alpha c_0} \ln \frac{1+\cos\theta(0)}{1-\cos\theta(0)}$$

and $\theta(z)$ decreases from $(\pi - \theta(0))$ to $\theta(0)$ between two consecutive reflections at $z = 0$. Simple calculations show that the rays are composed of arcs of circles with centres lying on the line $z = -1/\alpha$.

To facilitate comparison with (5.6) we can also write

$$d\tau = \frac{\sin \theta_1}{c_0(1+\alpha z_1)} dx - \frac{\cos \theta(z)}{c_0(1+\alpha z)} dz,$$

which gives for example for $n = 0$

$$\begin{aligned} \tau &= \lambda x - \frac{1}{\alpha c_0} \left[\int_{w_1}^1 - \int_w^1 \right] \frac{(1-\beta^2)^{1/2}}{\beta} d\beta, \quad \text{if } 0 < \theta_1 < \pi/2, \\ &= \lambda x + \frac{1}{\alpha c_0} \left[\int_{w_1}^1 \pm \int_w^1 \right] \frac{(1-\beta^2)^{1/2}}{\beta} d\beta, \quad \text{if } \pi/2 < \theta_1 < \pi, \end{aligned}$$

where $w = \lambda c$ and the upper sign is used if the ray has passed its turning point.

In (5.6) in $0 \leq z \leq z_1$

$$\tau_1 = v x - \frac{1}{\alpha c_0} \left[\int_{w_1}^1 - \int_w^1 \right] \frac{(1-\beta^2)^{1/2}}{\beta} d\beta$$

and

$$\tau_2 = v x + \frac{1}{\alpha c_0} \left[\int_{w_1}^1 + \int_w^1 \right] \frac{(1-\beta^2)^{1/2}}{\beta} d\beta$$

where v is the solution of respectively

$$vc_0 + \alpha x = [1 - (vc_0)^2(1+\alpha z)^2]^{1/2} - [1 - (vc_0)^2(1+\alpha z_1)^2]^{1/2}$$

and
$$vc_0 + \alpha x = [1 - (vc_0)^2(1+\alpha z)^2]^{1/2} + [1 - (vc_0)^2(1+\alpha z_1)^2]^{1/2}.$$

These equations can indeed be solved by substituting

$$vc_0 = \frac{\sin \theta_1}{1+\alpha z_1} = \frac{\sin \theta(z)}{1+\alpha z}.$$

We can also introduce ray coordinates (θ_1, τ) and rewrite the equation for $u_0^{(n)}$ as

$$\frac{2}{c^2} \frac{\partial u_0^{(n)}}{\partial \tau} + \frac{u_0^{(n)}}{Ic} \frac{\partial (I/c)}{\partial \tau} = 0,$$

where $I d\theta_1$ is the length of wave front between two adjacent rays.

This equation is solved by

$$u_0^{(n)} = \psi_0^{(n)}(\theta_1) (c/I)^{1/2}.$$

When $n = 0$
$$I = \frac{(\partial x / \partial \theta_1)}{\cos \theta} = \frac{1+\alpha z_1}{\alpha} \frac{\cos \theta - \cos \theta_1}{\sin^2 \theta_1}.$$

Near the source for small τ
$$I \sim \frac{\tau c \cos \theta_1}{\cos \theta}.$$

In this region $u_0^{(0)} f_0$ must be asymptotically equal to the elementary solution of our problem in a homogeneous medium

$$\frac{1}{2\pi} \frac{H(t-R/c)}{(t^2 - R^2/c^2)^{1/2}}$$

and we obtain

$$\psi_0^{(0)}(\theta_1) = 2^{-3/2} \pi^{-1/2}.$$

The amplitudes of the reflected waves follow from the boundary condi-

tion at $z = 0$ as

$$u_0^{(n)}(x,z) = 2^{-3/2} \pi^{-1/2} (c/I)^{1/2}.$$

Caustics are given by the curves $I = 0$.

Various pictures of the rays and wave fronts have been plotted by the computer and are shown in figures 6, 7 and 8.

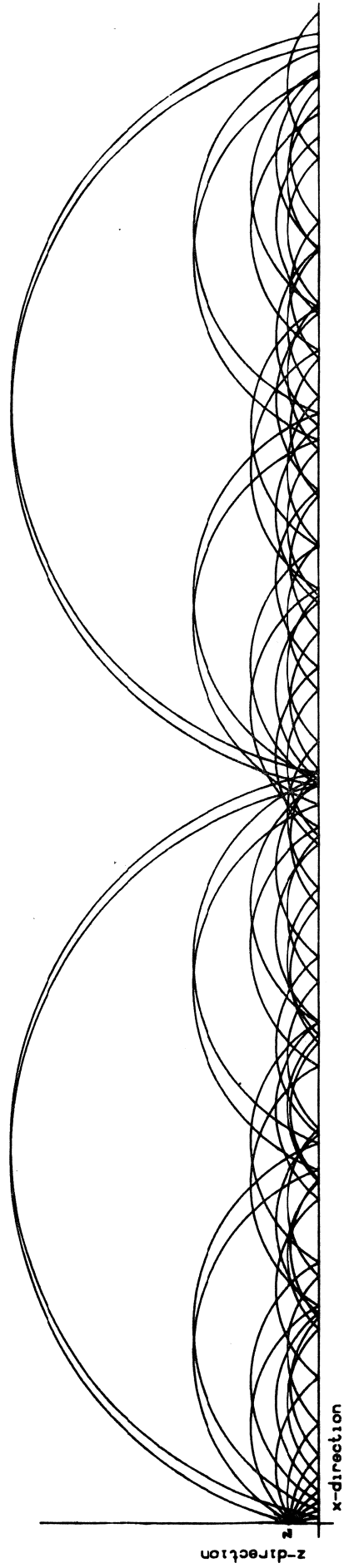
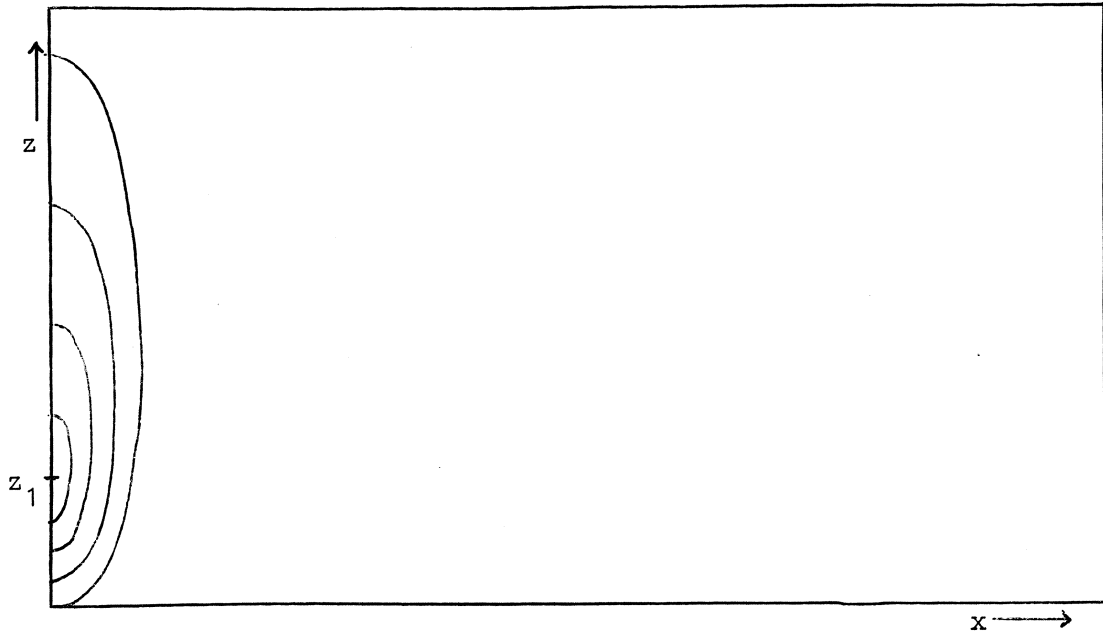
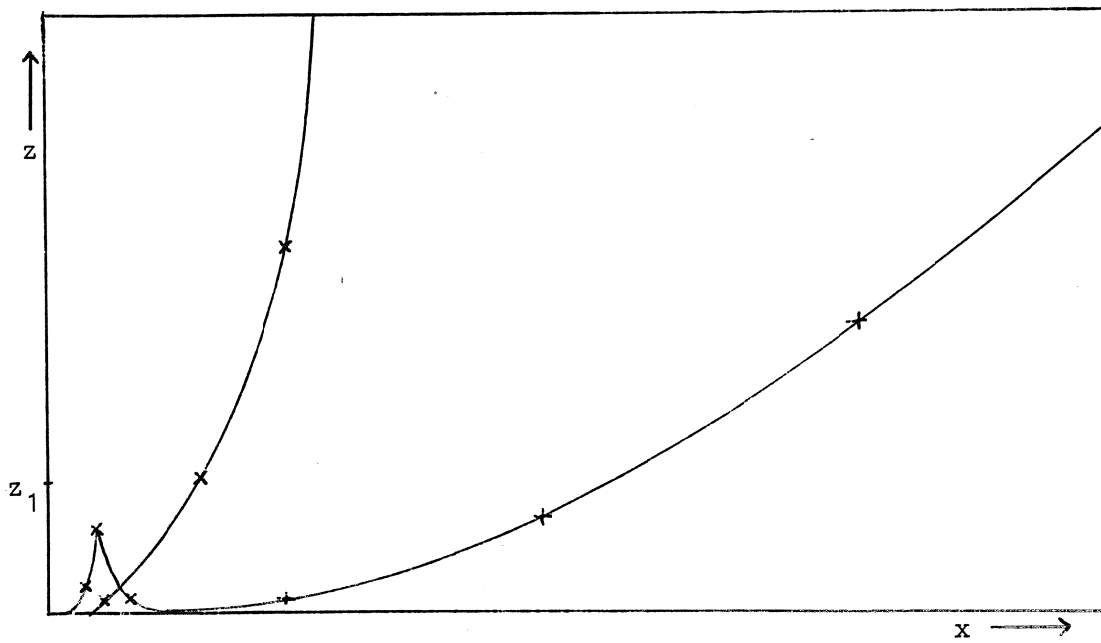


Figure 6. The ray picture.

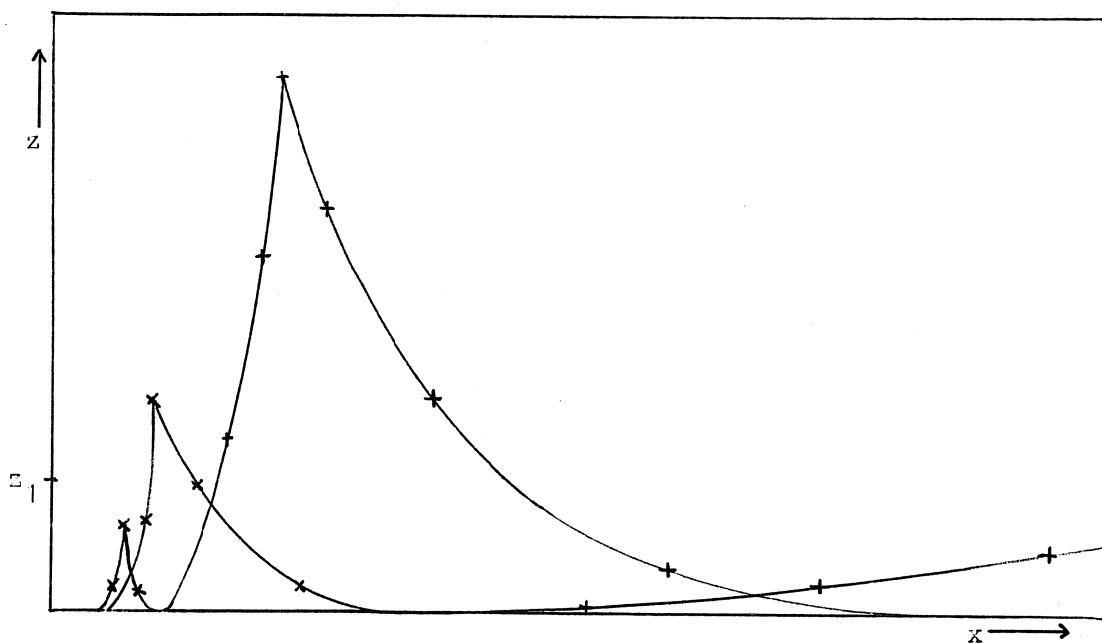


The development of the wave fronts as time goes from 0 to $\frac{1}{\alpha c_0} \ln(1 + \alpha z_1)$.

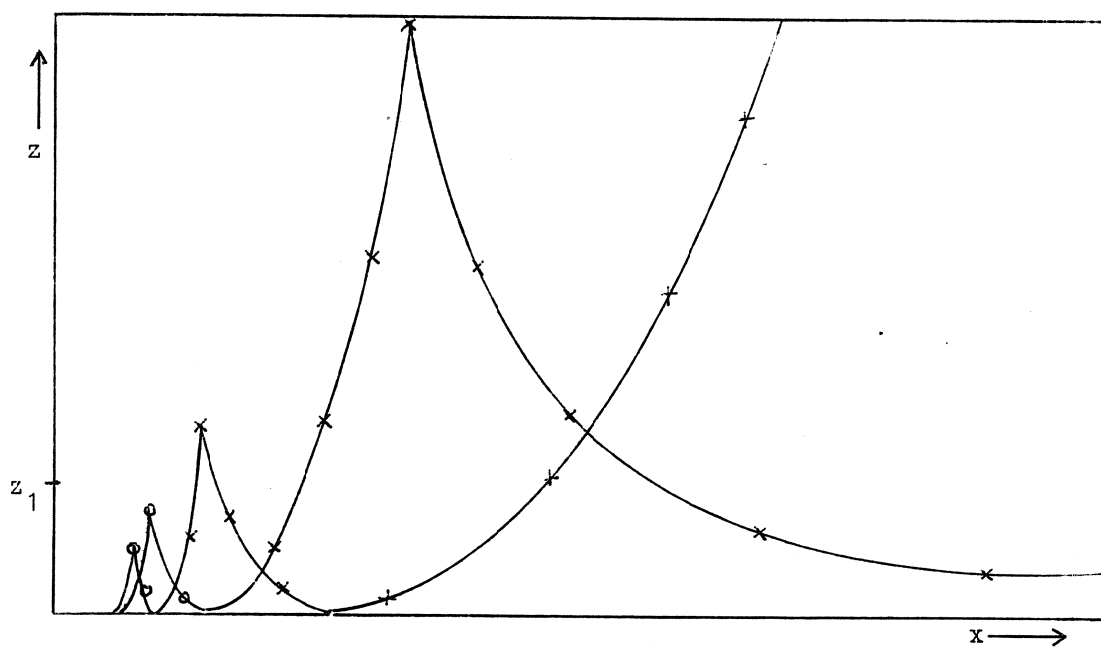


The wave fronts of the incoming (+) and the once-reflected wave at the moment when the second reflection starts.

Figure 7. Some wave fronts.



The wave fronts of the once (+)- and twice (x)-reflected wave at the moment when the third reflection starts.



The wave fronts of the once (+)-, twice (x)- and thrice (o)-reflected wave at the moment when the fourth reflection starts.

Figure 8. Some wave fronts.

Appendix 5. Details of the saddle-point calculations

For completeness we note that the expansion of U^* on $v = te^{\frac{i\pi}{2}i\phi}$, $-\infty < t < \infty$, is

$$\begin{aligned} \frac{is}{2\pi} e^{-vsx} U^* &\sim c \sum_{j=1}^6 g_j e^{-sf_j} [1 + o(s^{-1})], & t_{A'} < t < t_A, \\ &\sim c [e^{-sf_1} + (1 \mp ie^{-sf_0})^{-1} (e^{-sf_3 \pm ie^{-sf_5}})] [1 + o(s^{-1})], \end{aligned}$$

$$t_{B'} < t < t_{A'}, \quad t_A < t < t_B,$$

$$\sim c [e^{-sf_1} + (1 \mp ie^{-sf_0})^{-1} e^{-sf_3 \mp ie^{-s(f_3 - f_0)}}] [1 + o(s^{-1})],$$

$$t_{C'} < t < t_{B'}, \quad t_B < t < t_C,$$

$$\sim c [e^{-sf_1} + e^{-sf_3}] [1 + o(s^{-1})],$$

$$-\infty < t < t_{C'}, \quad t_C < t < \infty,$$

where
$$c = \frac{c_0(1+\alpha z_1)}{4\pi i} \chi(1-w_1^2)^{-1/4} (1-w^2)^{-1/4}$$

and g_j, f_j ($j=1,2,\dots,6$) are given in (4.1). See figure 1.

Along $v = te^{\frac{i\pi}{2}i\phi}$, $0 < t < \infty$, we can use Laplace's method [4] to

obtain estimates for integrals of the kind $\int_{t_1}^{t_2} g_j e^{-sf_j} dt$ as all $\operatorname{Re} sf_j$

are monotonous functions of t . Specifically, $\operatorname{Re} sf_1, \operatorname{Re} sf_3$ and $\operatorname{Re} s(f_3 - f_0)$ increase with t and show a relative minimum at the lower end point of the interval, while the other functions decrease with t and take their minimum value at the higher end point of the interval. Therefore

$$\int_{t_1}^{t_2} g_j e^{-sf_j} dt \sim O(s^{-1} \exp(-sf_j)) = o(s^{-1}),$$

because $\operatorname{Re} sf_j > 0$ at the endpoint in question.

This information can be considered sufficient for our purpose. The exponential factors correspond to time shifts in the original pulse propagation problem, while the algebraic factor is directly related to the shape of the pulse and its amplitude. The saddle point and pole contributions all contain factors $s^{-\beta}$, $0 < \beta < 2/3$, and are therefore connected with disturbances which are more important.

Again restricting our attention to $0 < \phi < \pi/2$ we remark that both saddle points and poles are located in $\operatorname{Im} vs > 0$. All integrals

along $v = te^{-i\frac{\pi}{2}-i\phi}$ can therefore be estimated as $o(s^{-1})$. In x, z -regions where f_j doesn't have a saddle point the same estimate will be used along $v = te^{i\frac{\pi}{2}-i\phi}$. The only exception is $j = 3$.

The different contours which have been used are shown in figure 9. We will not give any of the calculations here, but only make some remarks. The results of the calculations are given in (4.3).

$j = 1$.

This is the most straight forward case. If there is a saddle point contour a is used. There is no contribution from the arc of circle at infinity.

$j = 2, 4, 6$.

The saddle point contour for these cases is shown in figure 9b.

$j = 3$.

If a saddle point occurs we use contour c . The poles may interfere however, which becomes noticeable when the path of steepest descent recrosses the positive real v -axis on $v_{s3} < v < v(0)$, see figure 9d. If there is no saddle point the poles must be taken into account (figure 9e).

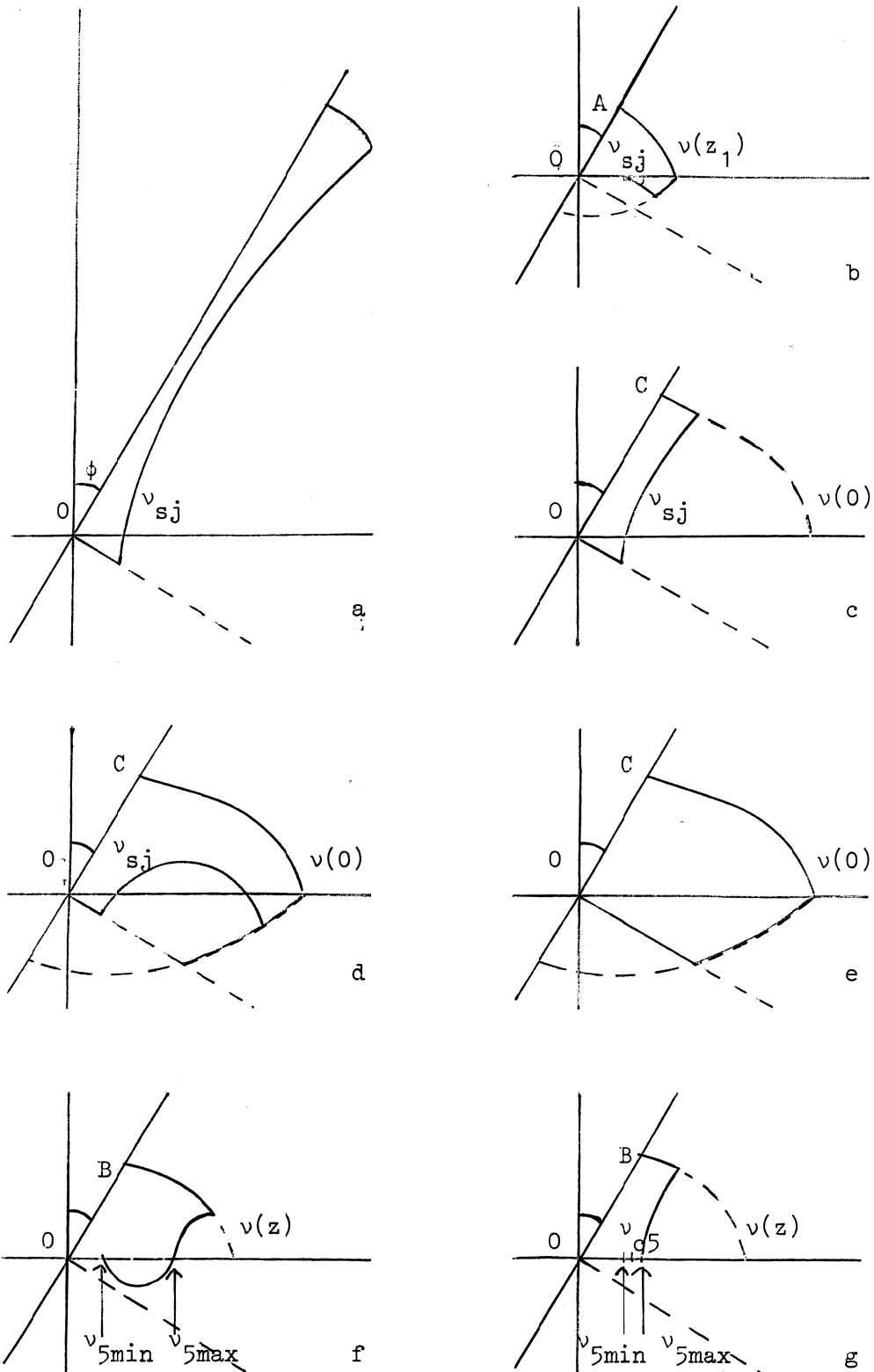


Figure 9. The path of integration in the v -plane.

j = 5.

If there is a single saddle-point we use contour b, where $v(z_1)$ must be replaced by $v(z)$ and A by B. If two saddle points occur which are well apart we use contour f. Near the caustic the contour of figure 9g will be used.

When (x,z) approaches one of the boundary curves we replace the relevant pair of exponentials by an Airy function on $0 < t < t_A$ and use contour b. Near the caustic of $f_{3,4}$ again contour g is used.

